#### Research Article

Yuanxun Zheng, Jingbo Zhuo, Yamin Zhang, and Peng Zhang\*

# Mechanical properties and microstructure of nano-SiO<sub>2</sub> and basalt-fiber-reinforced recycled aggregate concrete

https://doi.org/10.1515/ntrev-2022-0134 received April 3, 2022; accepted May 18, 2022

Abstract: In this study, nano-SiO<sub>2</sub> (NS) and basalt fiber (BF) were used to improve the quality of recycled aggregate concrete (RAC). The crushing value, water absorption, and apparent density of NS-modified recycled coarse aggregate (RA) were determined, and the effects of BF with different contents and lengths on the slump, compressive strength, splitting tensile strength, and flexural strength of RAC and BF-reinforced RAC containing NS-modified RA were analyzed. Finally, the filling effect of NS, the toughening and crack resistance mechanism of BF, and the micro-composite effect between NS and BF were analyzed based on scanning electron microscope (SEM) and energy-dispersive detector (EDS) measurement. The results show that the optimum modified concentration of NS solution is 2%, the content of BF is the main factor affecting the mechanical properties of concrete, and the optimum length and content of BF are 12 mm and 0.2%, respectively. For BF-reinforced RAC containing NS-modified RA, the 28 day compressive strength, splitting tensile strength, and flexural strength of RAC increase by 34.28, 40.55 and 54.5%, respectively. Based on SEM and EDS measuring, NS can react with Ca(OH)<sub>2</sub> crystal to form flocculent C-S-H gel, which makes RAC compact and enhances the bonding properties of the interfacial transition zone (ITZ) between BF and the matrix.

**Keywords:** recycled aggregate concrete, nano-SiO<sub>2</sub>, basalt fiber, mechanical properties

Yuanxun Zheng, Jingbo Zhuo: School of Water Conservancy Engineering, Zhengzhou University, Zhengzhou, 450001, China Yamin Zhang: Library, Zhengzhou University, Zhengzhou, 450001, China

#### 1 Introduction

As the largest amount of artificial building materials, concrete has a severe adverse impact on natural resources and the environment [1,2]. Meanwhile, the rapid growth of the construction industry has produced a great quantity of building waste, which is rising with each passing year [3,4]. Therefore, the effective use of construction waste to produce recycled aggregate concrete (RAC), reduce the mining of traditional concrete materials, and develop green buildings are major problems that must be solved in today's society [5]. The emergence of RAC points out a sustainable development path for the solution of construction waste [6,7]. However, compared with natural aggregate concrete (NAC), the performance of RAC is poor because there is a lot of adhered mortar on RA, which makes RA have defects of high porosity and high water absorption [8,9]. During the mixing process of RAC, the existence of attached mortar will cause multiple complex interfacial transition zone (ITZ) in the RAC mixed with RA [10,11], which will make the natural defects such as high brittleness, low tensile strength, easy shrinkage, and cracking of concrete more prominent, resulting in the poor deformability, mechanical properties, durability, and impermeability of RAC than NAC [12,13]. Therefore, to enhance the utilization of RA, the application domain of RAC is promoted. It is of practical significance for the development of RA and RAC to study the economical and efficient strengthening method of RA [14,15].

To promote the use of RAC, some researchers [16–18] have studied the modification of RA. Compared with physical strengthening and microbial strengthening, chemical methods such as chemical reagent soaking method and nanomaterial soaking method have the characteristics of good performance and easy adhesion to the surface of mortar and aggregate [19,20], which can effectively fill the porous medium with permeability [21,22]. Compared with nanomaterials such as nano-TiO<sub>2</sub> and nano-CaCO<sub>3</sub> [23], NS has significant advantages [24,25]. For example, NS can easily react with the residual CH in RA to stimulate the

<sup>\*</sup> Corresponding author: Peng Zhang, School of Water Conservancy Engineering, Zhengzhou University, Zhengzhou, 450001, China; Yellow River Laboratory, Zhengzhou University, Zhengzhou, 450001, China, e-mail: zhangpeng@zzu.edu.cn

activity of RA and pad the holes, thus improving the water absorption and porosity of RA [26]. Various advantages make NS-modified RAC become a hot research topic [27–29]; however, there are excessive NS granules on the RA due to pre-soaking, which has an adverse impact on the structure of ITZ [30,31]. Therefore, more research is needed on the dose of NS, soaking time, *etc*.

In addition, with the development of nanomaterial technology, nanomaterials are becoming more and more affordable [32,33]. The price of NS solution (30% by mass) used in the test is RMB 5,000 (about US\$750) per ton [34,35]. Several studies have shown that the consumption of nanoparticles is very small in the modification process of concrete, and the cost of using each cubic meter of concrete is about RMB 65 (about US\$10) [36,37]. Therefore, in this study, RA was strengthened by NS suspension, and the improvement in the physical properties of RA and the mechanical properties of RAC was compared before and after strengthening, providing a theoretical basis for resource utilization of RA.

Through the use of modified RA, the compressive strength of RAC can be effectively improved, and RAC can be widely used [38]. However, strengthening RA will not eliminate the defects of concrete like high brittleness and low tensile strength [39]. To enhance the brittleness of concrete, researchers added steel fiber [40,41], polypropylene fiber [42], PVA fiber [43,44], nylon fiber [45], and basalt fiber (BF) into concrete to prepare fiber concrete, which can effectively improve the anti-cracking ability and enhance the ductility, thus improving the mechanics and durability of concrete [46]. The appearance of fibers provides a new idea for the development of RAC [47,48]. Compared with other fibers, BF has the advantages of high strength, corrosion resistance, good silicate compatibility, and thermal expansion coefficient similar to concrete. At the same time, the small diameter of BF can effectively reduce the occurrence and development of early microcracks [49–51]. According to Katkhuda and Shatarat [52], Fang et al. [51], and Zheng et al. [53], when the content of BF is in the range of 0-0.3%, BF can enhance the mechanical properties of RAC. Wang et al. [54] and Hassani et al. [55] concluded that when BF of appropriate length is added to the concrete, the crack propagation can be effectively prevented and the toughness of the concrete can be improved. Therefore, this study intends to reveal the effect of the length and content of BF on the mechanical properties of RAC, so as to provide theoretical basis and optimal content for the application of RAC.

Related results show that compared with the single addition of nano-materials and fibers, the combination of them can prepare RAC with high mechanical strength [54,56]. Therefore, to enhance the mechanical properties of RAC composites, especially the flexural strength, to meet the needs of engineering practice, investigators have done more research work on RAC [57]. However, the related research results on the mechanical properties of BF-reinforced RAC containing NS-modified RA are limited. Therefore, in view of the low comprehensive utilization rate of RAC, this study intends to combine macro-experimental research and micro-mechanism analysis to systematically study the performance improvement mechanism of BF-reinforced RAC containing NS-modified RA. In view of this, this study intends to provide a theoretical basis for the design and application of RAC.

# 2 Experimental investigation

#### 2.1 Raw materials

The RA used in this study was from Xuchang Jinke Resources Recycling Co., Ltd, which was prepared from crushed waste concrete. The crushed waste concrete was screened by two screens with a maximum pore size of 20 mm and a minimum pore size of 4.75 mm, and the fragments between 5 and 20 mm were taken as RA. The particle size distribution of RA is shown in Figure 1. The performance indices of recycled coarse aggregate were tested according to the standard of "Pebble and crushed stone for construction" (GB/T14685-2011) and "Recycled coarse aggregate for concrete" (GB/T25177-2010). The fine aggregate was natural river sand with a fineness modulus

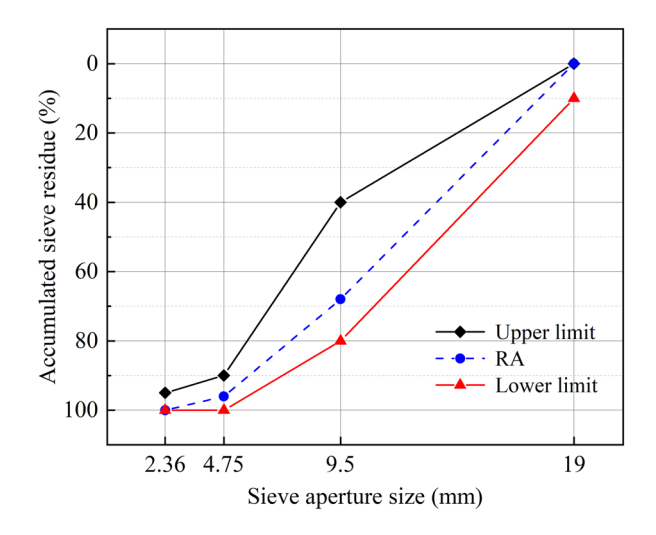


Figure 1: Gradation curve of RA.

Table 1: Properties of RA and sand

Туре	Particle size (mm)	Apparent density (kg/m³)	Water absorption (%)	Crushed value (%)	Porosity (%)	
RA	5–20	2,550	5.3	16.3	49.6	
Sand	0-5	2,465	0.61	_	_	

Table 2: Properties of cement

	Specific surface area (m²/kg)	Initial setting time (min)	Final setting time (min)	Boiling stability	3D compressive strength (MPa)	3D flexural strength (MPa)
	≥300	≥45	≤600	Qualified	≥17	≥3.5
Measured value	352	165	220	Qualified	23.5	5.6

Table 3: Properties of BF

Density (kg/m³)	Single dimension diameter (µm)	Length (mm)	Tensile strength (MPa)	Elastic modulus (GPa)
2.65	13	6, 12, and 8	3,000-4,800	91–110

of 2.67, which can be classified as medium coarse sand. The properties of fine aggregate were tested according to the standard of "Sand for construction" (GB14684-2011). The properties of RA and fine aggregate are shown in Table 1. PO 42.5 ordinary Portland cement is adopted, and the performance indices of the cement are in line with the performance indices specified in the Code "General Portland cement" (China GB175-2007). The performance index of cement and its strength at the age of 3 days are shown in Table 2. Nano-SiO2 solution was a HTSi-11L solution produced by Nanjing Haitai Nano Materials Co., Ltd, with a concentration of 30%. A polycarboxylic acid high-performance water reducing agent is adopted with a water reduction rate of 25%. Tables 3-4 show the physical properties of NS and BF.

#### 2.2 Design of mixture proportions

The chemical strengthening procedure of RA is as follows. First, the RA was cleaned and air-dried, then soaked in a uniformly dispersed NS solution with concentrations of 0,

Table 4: Properties of NS

Color	Content (%)	Particle size (nm)	рН	Purity (%)	
White	30	15-30	9-10	≥99	

1, 2, and 3%, respectively, and finally dried. The soaking time is designed to be 48 h, and the atmospheric soaking process of RA is shown in Figure 2. Before the test block was mixed, physical performance indicators of RA were tested according to "Technical Requirements and Test Method of Gravel and Crushed Stone for Ordinary Concrete" (JGJ53-92). The best modified concentration of NS was obtained, as shown in Table 5.

The mix ratio of this study is designed according to the "Code for mix proportion Design of ordinary concrete" (China JGJ 55-2011). As shown in Table 6, the water-cement ratio is 0.51, the sand ratio is 36%, the replacement rate is 100%, and the particle size is 5-20 mm. Unmodified RA and RA after soaking in NS solution were selected to mix RAC. The length of BF is designed as6, 12, and 18 mm, and the volume content of BF is designed as 0, 0.1, 0.2, and 0.3%, respectively.

#### 2.3 Sample preparation

The RAC preparation flow chart is shown in Figure 3. After completing the mixture, the slump was measured. After the completion of casting and demolding of the samples, the sample should be immediately moved to the standard concrete curing room where the temperature and humidity are constant at 20  $\pm$  2°C and the relative humidity is not less than 95%.

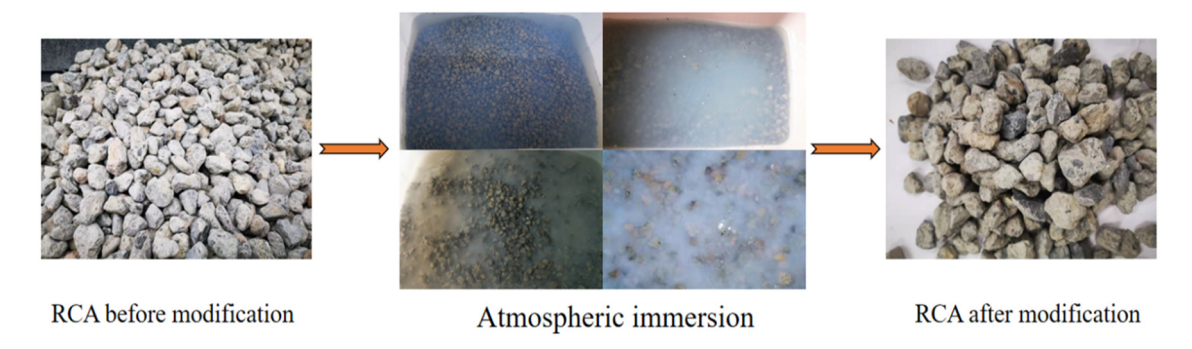


Figure 2: Schematic diagram of RA soaked in nano-SiO<sub>2</sub> at atmospheric pressure.

Table 5: Effect of NS on physical properties of RA

Aggregate category	Crushing value (%)	Water absorption (%)	Apparent density (kg/m³)	
RA-NS0	14.85	6.52	2,550	
RA-NS1	11.69	5.61	2,564	
RA-NS2	10.42	4.66	2,593	
RA-NS3	11.42	4.98	2,589	

#### 2.4 Experimental methods

In this study, the RAC mix ratio under 22 working conditions was designed. As shown in Table 7, 198 specimens were poured to determine the 28 day mechanical properties of RAC. The sizes of the specimens were  $100~\text{mm} \times 100~\text{mm} \times 100~\text{mm} \times 100~\text{mm} \times 100~\text{mm} \times 100~\text{mm} \times 100~\text{mm}$ , and  $100~\text{mm} \times 100~\text{mm} \times 400~\text{mm}$ .

The mechanical tests were implemented according to the "Standard for test methods of concrete physical and

Table 6: Proportion of mixture and various mechanical properties

Group	Mixture proportion (kg/m <sup>3</sup> )					Admixture		Slump	Mechanical properties (28 day, MPa)		
	Water	er Cement	Sand	RA	Water reducing agent	BF		(mm)	Compressive	Splitting	Flexural
						Length (mm)	Content (%)		strength	tensile strength	strength
NS0BF0	210	415	617	1,148	4.2	0	0	110	27.19	2.17	3.52
NS1BF0	210	415	617	1,148	4.2	0	0	104	29.97	2.26	3.81
NS2BF0	210	415	617	1,148	4.2	0	0	95	32.50	2.50	4.12
NS3BF0	210	415	617	1,148	4.2	0	0	84	31.80	2.46	4.00
NS0BF6-1	210	415	617	1,148	4.2	6	0.1	95	25.97	2.22	3.80
NS0BF6-2	210	415	617	1,148	4.2	6	0.2	89	29.57	2.48	4.14
NS0BF6-3	210	415	617	1,148	4.2	6	0.3	76	24.75	2.59	4.12
NS0BF12-1	210	415	617	1,148	4.2	12	0.1	105	26.22	2.28	3.90
NS0BF12-2	210	415	617	1,148	4.2	12	0.2	96	30.25	2.58	4.51
NS0BF12-3	210	415	617	1,148	4.2	12	0.3	82	23.79	2.67	4.16
NS0BF18-1	210	415	617	1,148	4.2	18	0.1	99	26.51	2.34	4.02
NS0BF18-2	210	415	617	1,148	4.2	18	0.2	87	29.98	2.66	4.65
NS0BF18-3	210	415	617	1,148	4.2	18	0.3	76	23.40	2.62	3.99
NS2BF6-1	210	415	617	1,148	4.2	6	0.1	82	31.12	2.55	4.45
NS2BF6-2	210	415	617	1,148	4.2	6	0.2	77	35.34	2.84	4.84
NS2BF6-3	210	415	617	1,148	4.2	6	0.3	65	29.58	2.97	4.82
NS2BF12-1	210	415	617	1,148	4.2	12	0.1	91	31.28	2.62	4.56
NS2BF12-2	210	415	617	1,148	4.2	12	0.2	83	36.51	2.96	5.28
NS2BF12-3	210	415	617	1,148	4.2	12	0.3	71	28.50	3.06	4.87
NS2BF18-1	210	415	617	1,148	4.2	18	0.1	85	31.68	2.68	4.70
NS2BF18-2	210	415	617	1,148	4.2	18	0.2	75	35.83	3.05	5.44
NS2BF18-3	210	415	617	1,148	4.2	18	0.3	65	27.97	3.01	4.67

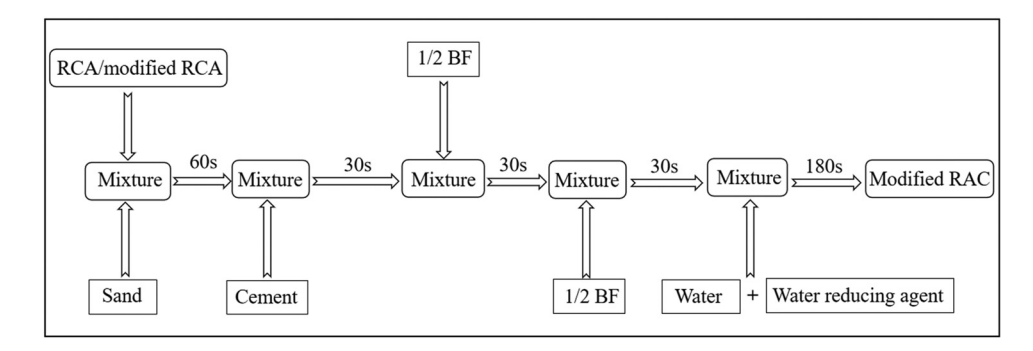


Figure 3: Determination process of crushing value of RA. (1) Sample and put into the mold; (2) apply load; (3) sieve the sample.

mechanical properties" (China GB/T50081-2019). Meanwhile, the micro-structure of RAC was analyzed through the tests of scanning electron microscope (SEM) and energy-dispersive detector (EDS).

## 3 Results and analysis

#### 3.1 Effect of NS on physical properties of RA

#### 3.1.1 Water absorption

One of the most obvious defects of RA is that it has higher water absorption than NCA, and the increased water absorption of RA means that RAC typically absorbs more water than NAC to achieve the same workability. Therefore, the use of RA in dry conditions leads to a decrease in the workability of concrete.

As shown in Table 5, when the concentration of NS solution was 1, 2, and 3%, the water absorption of RA reduced by 13.96, 28.53, and 23.62%, respectively. Shaikh et al. [38] got similar results. This phenomenon is related to the good dispersion and high activity of NS. There were some pores filled by C-S-H gel on the surface of RA, which improved the internal structure of RA and the properties of adhered mortar, thus the water absorption can be reduced and the overall quality of RA can be improved. However, when the NS solution was 2-3%,

the water absorption of RA remained basically unchanged. There are some related reasons for the experimental phenomenon. First, under the condition of atmospheric pressure immersion, the speed of NS entering the aggregate slows down. The agglomeration of NS particles blocks some pores, thus affecting the modification effect of NS on RA. Second, when the concentration of NS solution is 1 and 2%, the water absorption of RA decreases rapidly because C-S-H gel fills the pores of aggregate, but with the depletion of CH in aggregate, the later modification effect of NS is mainly to fill micro-cracks, and the filling speed is much lower than that of the former. In summary, considering the strengthening effect of NS on RA and economic factors, 2% concentration of NS solution is the optimal dosage.

#### 3.1.2 Crushing value

Crushing value is a performance index to measure the resistance of aggregate to pressure, and an important index to measure the quality of RA. According to the specification requirements, 10 kg of RA with a particle size of 9.5-19 mm were measured and evenly divided into three parts. Each group of RA was added into the compression mold twice, and each was loaded with a layer up and down 25 times until the aggregate surface was smooth. Then, the aggregate was loaded at a rate according to the specification. Finally, a screen with a diameter of 2.36 mm was used to remove the crushed

Table 7: Design of the experiment

Static mechanical property test	Group	Sizes of specimen (mm)	Number of specimens	Curing period (days)
Compressive strength	22	$100\times100\times100$	66	28
Splitting tensile strength	22	$100\times100\times100$	66	28
Flexural strength	22	$100\times100\times400$	66	28







Figure 4: Determination process of crushing value of RA. (1) Sample and put into the mold; (2) Apply load; (3) Sieve the sample.

fine particles, and the crushing value was calculated according to the formula. This procedure was repeated three times, and the average value of the three tests was taken as the final result. The testing process of crushing value of RA is shown in Figure 4.

Table 5 reflects the modification law of the concentration of NS solution, in which the strengthening effect is the best when the concentration of NS solution is 2%. When the concentration of NS solution is 1, 2, and 3%, the crushing value of RA decreases by 21.28, 29.85, and 23.10%, respectively. Zhang *et al.* [39] got the same conclusion. The crushing value indices were significantly reduced by NS, mainly because the flocculent gel formed during immersion fills the micropores of RA and improves the strength of RA.

#### 3.1.3 Apparent density

Apparent density refers to the mass per unit volume of aggregate in the natural state, which can indirectly reflect the compactness of aggregate. For the same batch of aggregates from the same source, with the decrease in porosity, the apparent density of aggregates increased, while the water absorption and crushing index decreased at the same time. When the source of aggregate was the same, the properties of aggregate were similar, and the crushing index, water absorption, and apparent density will decrease or increase regularly [58]. Related results showed that the apparent density of RA was lower than that of NCA due to the adhered mortar, which was mainly because there were many pores in the old mortar indicated by RA, and even some RA particles were completely mortar particles [59]. In addition, different types and amounts of modifiers also have some effects on the apparent density of RA.

As shown in Table 5, the apparent density of RA modified by NS solution continues to increase, and the enhancement effect is optimal when the NS solution

concentration is 2%. When NS solution concentration is 1, 2, and 3%, the apparent density of RA increases from 2,550 to 2,564, 2,593, and 2,589 kg/m³, respectively. The experimental results showed that some cracks in RA were filled and repaired in the process of strengthening, thus improving the apparent density of RA.

#### 3.2 Slump

So far, there is no single index to comprehensively reflect the workability of concrete. Usually, it is mainly based on the determination of the slump of concrete, supplemented by other intuitive observation or comprehensive evaluation by experience [60]. As shown in Table 6 and Figure 5, the slump diminishes with the increase in the concentration of NS solution. Because there are unreacted NS particles on the surface of RA, the dry NS particles will absorb free water, which decreases the fluidity of RAC. Meanwhile, the high water absorption capacity of RA reduces the workability of concrete mixture, and the existence of NS powder further reduces the fluidity of RAC. When the concentration of NS solution is 1 or 2%, it has

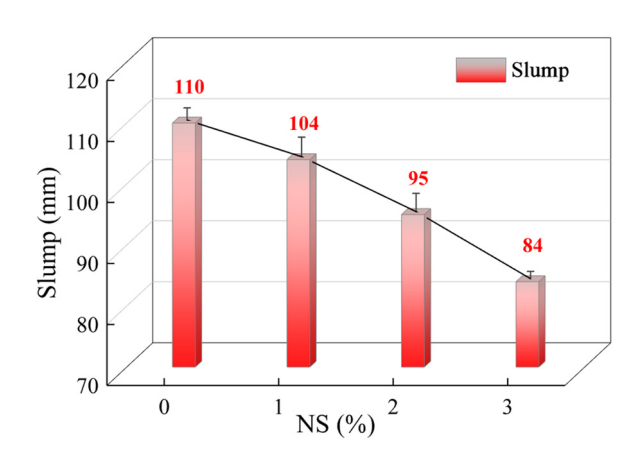


Figure 5: Effect of NS concentration on the slump of RAC.

a slight influence on the slump of RAC. Because most NS particles are consumed to improve the porosity of RA, there are fewer NS particles attached to the surface of aggregate. When the concentration of NS solution is 3%, a large number of NS particles lead to the obvious decrease in the slump of RAC.

As shown in Figure 6, the increase in the length and content of BF has an adverse effect on the fluidity of RAC. For the content of BF, the slump decreases slightly between 0-0.1%, but the effect on fluidity is not significant. When the content of BF is 0.1-0.2%, the slump decreases significantly. When the content of BF is more than 0.2%, RAC basically loses fluidity, and the slump of RAC changes little. The effect of the length of BF on the fluidity of concrete is related to the content of BF, and it has an insignificant effect on the fluidity at a low content. However, the effect of the length and content of BF on the fluidity is positively correlated. The length of BF has an obvious effect at high content; that is, the fluidity of concrete is influenced by the content and length of BF. Besides, the slump of concrete decreases most significantly at a short length. This is because the length of 6 mm BF is shorter, the contact area with water is larger, and the wrapped water is the most, which results in the most significant drop in slump.

#### 3.3 Compressive strength

According to Table 6 and Figure 7, the compressive strength of RAC prepared by pre-soaking RA at 2% concentration increased by 19.53%, while that at 3% concentration

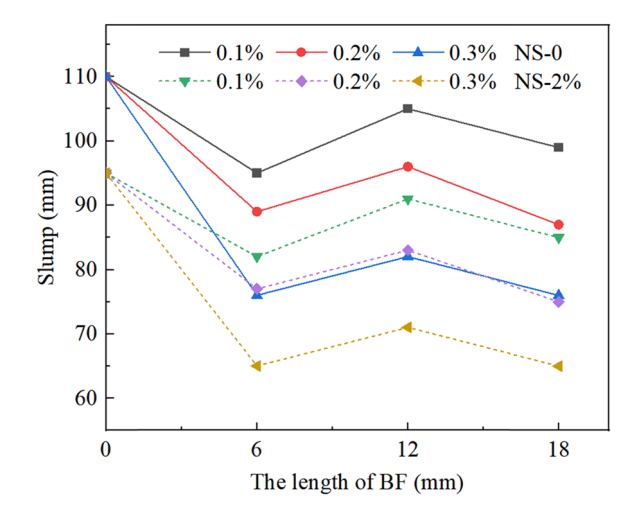


Figure 6: Effects of the length and content of BF on the slump of RAC.

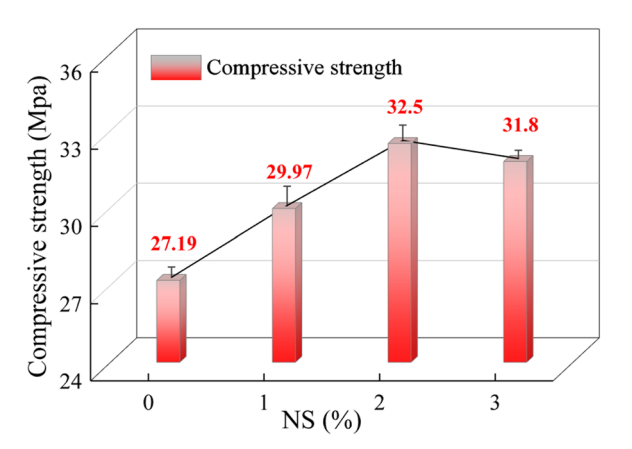


Figure 7: Effect of NS concentration on the compressive strength of RAC.

increased by 16.95%. When the concentration of NS solution is low, NS promotes the hydration of cement, and the resulting C-S-H gel can fill in the micropores and microcracks of RAC. However, with the increase in the concentration of NS solution, NS particles in the aggregate pores are saturated, which affects the NS particles entering the interior of the aggregate, resulting in a relatively poor modification effect of RA. When the concentration of NS solution is 3%, NS particles on adhered mortar can attract surrounding water molecules to form silane alcohol groups (Si-OH) on the surface of adhered mortar, which makes RAC absorb free water during mixing, resulting in a decrease in fluidity and affecting the working performance of RAC to a certain extent.

Figure 8(a) shows that the optimum content of 28 day compressive strength of BFRAC is 0.2%. When the content of BF is 0.1%, the bridging effect of BF cannot be fully exerted, which affects the compactness of RAC matrix and results in the reduction in strength. With the addition of appropriate content of BF, a randomly distributed support system was formed in RAC, which reduces the porosity of RAC, restrains the development of microcracks in the matrix, and then improves the integrity of RAC. However, when excessive BF is added, the BF interferes with each other, resulting in the serious agglomeration and a decrease in compressive strength. As shown in Figure 8(b), when the length of BF is 12 and 18 mm, the improvement in the compressive strength of RAC is better than that of 6 mm. Because under the premise of uniform dispersion, the longer the length of BF, the less likely it is to be pulled out under the action of force. Considering the effect of the length and content of BF, it can be concluded that 12 mm or 18 mm is the optimal length choice, and when the content of BF is 12-0.2%, the 28 day

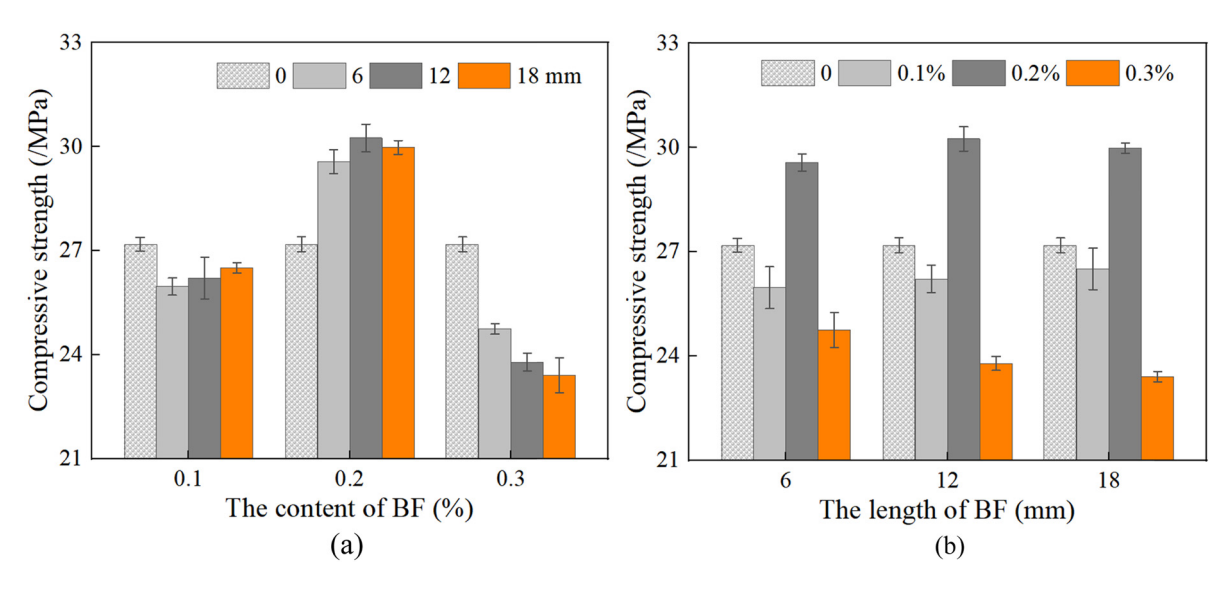


Figure 8: Effect of BF on the compressive strength of RAC. (a) RAC with different BF contents. (b) RAC with different BF lengths.

compressive strength of BFRAC is 11.25% higher than that of ordinary RAC. Iyer *et al.* [61] and Nihat *et al.* [49] got similar results.

As shown in Table 6 and Figure 9, for BF-reinforced RAC containing NS-modified RA, compared with adding BF alone, the 28 day compressive strength of RAC is enhanced. In the absence of NS, the ITZ of BF is loose, and there are many loose and porous flake crystals in RAC. With the addition of NS, there are a large number of unsaturated bonds in the NS particles on the surface of RA, which will promote the hydration of cement and form a uniform and dense C-S-H gel with NS particles as the core. And its huge specific surface area is beneficial to promoting the performance of the new and old ITZ of RA. Meanwhile, the flocculent C-S-H gel is closely connected with the compound, which strengthens the adhesion between the matrix and BF, and enhances the properties of ITZ between the fiber and cement matrix. In conclusion, for BF-reinforced RAC containing NS-modified RA, the optimal concentration of NS solution is 2%, the best length and content of BF are 12 mm and 0.2%, and the 28 day compressive strength is improved by 34.28%.

#### 3.4 Splitting tensile strength

As can be seen from Table 6 and Figure 10, compared with unmodified RAC, the splitting tensile strength of RAC modified by 1, 2, and 3% NS solution increases by 7.37, 14.75, and 13.36%, respectively, indicating that there is an optimal modification concentration of NS solution. Furthermore, ITZ is a significant factor affecting the splitting tensile strength

of concrete. After being modified by NS solution, C–S–H gel is formed on ITZ, which densifies the ITZ of RAC and forms stronger chemical bonds, so the splitting tensile strength is improved. However, excessive NS particles have an adverse effect on the viscosity of cement mortar and reduce the increase in splitting tensile strength. Considering the modification effect and cost, the modification of RA with 2% NS solution is the best choice.

According to Figure 11(a), the splitting tensile strength of RAC is positively correlated with the content of BF. When the content of BF is less than 0.2%, the uniformly dispersed BF makes up for the defects in the internal structure and enhances the compactness and integrity of RAC.

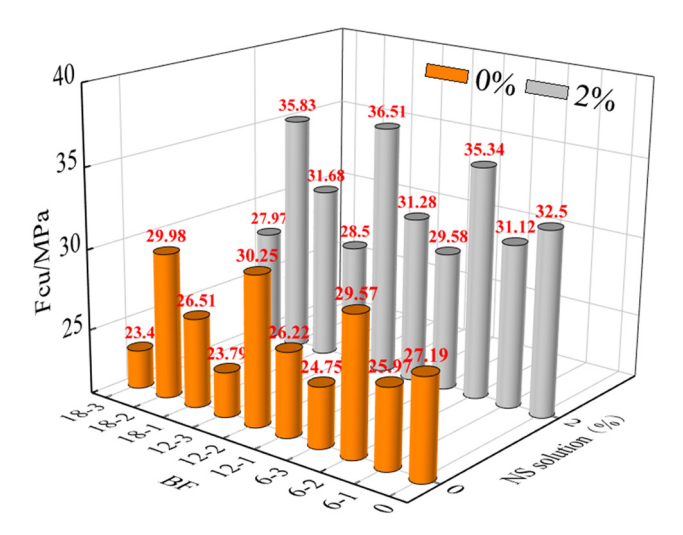


**Figure 9:** The synergistic effect of NS and BF on the compressive strength of RAC.

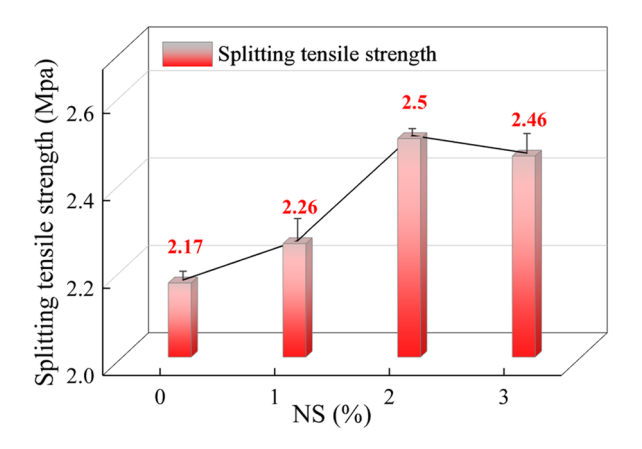


Figure 10: Effect of NS concentration on the splitting tensile strength of RAC.

However, when the content of BF is 0.3%, BF agglomerates in the mixing process, resulting in the poor ITZ between BF and cement matrix, and then the improvement of splitting tensile strength decreases. According to Figure 11(b), when the length of BF is 6 mm, the length is too short so that it is easy to be pulled out in the process of stress, so the strengthening effect is not significant. This phenomenon was confirmed by the study by Kou et al. [62] and Chen et al. [63]. With the increase in the length of BF, a part of BF is completely wrapped in cement matrix, which can promote the compactness of RAC. Another part of BF can penetrate the pores and microcracks of RAC and effectively improve the internal structure of RAC.

For BF-reinforced RAC containing NS-modified RA, the NS particles on the RA surface enhanced the performance of the ITZ of RAC, which provided more nucleation sites for C-S-H gel, enhanced the bonding force between the matrix and BF, and enhanced the bridging effect of BF. According to Figure 12, when the concentration of NS is 2%, and the length and content of BF are 18 mm and 0.2%, respectively, the modification effect of RAC is the best. Compared with unmodified RAC, the 28 day split tensile strength increased by 40.55%.

#### 3.5 Flexural strength

As can be seen from Figure 13, when the concentration of NS is 1, 2, and 3%, the flexural strength of 28 day increases by 8.4, 16.96, and 13.51%, respectively, which effectively improves the flexural performance of RAC. NS particles reduce the critical pore size and porosity of RA by promoting the hydration reaction of cement, which makes the internal structure of RA more compact, and thus improves the comprehensive properties of RA. In addition, NS enhances the strength of ITZ between RA and cement matrix, thus improving the flexural strength of RAC. However, when the immersion concentration of NS is 3%, NS particles will not play an effective filling role and crystal nucleus effect, which affects the flexural performance.

As shown in Table 6 and Figure 14, when the content of BF is between 0.1 and 0.3%, there is optimal content to enhance the flexural strength of RAC. When the content of BF is low, the growth rate of flexural strength increases continuously. When the content is more than 0.2%, the improvement effect of BF is worse. The mechanical strength of RAC can be improved most effectively by

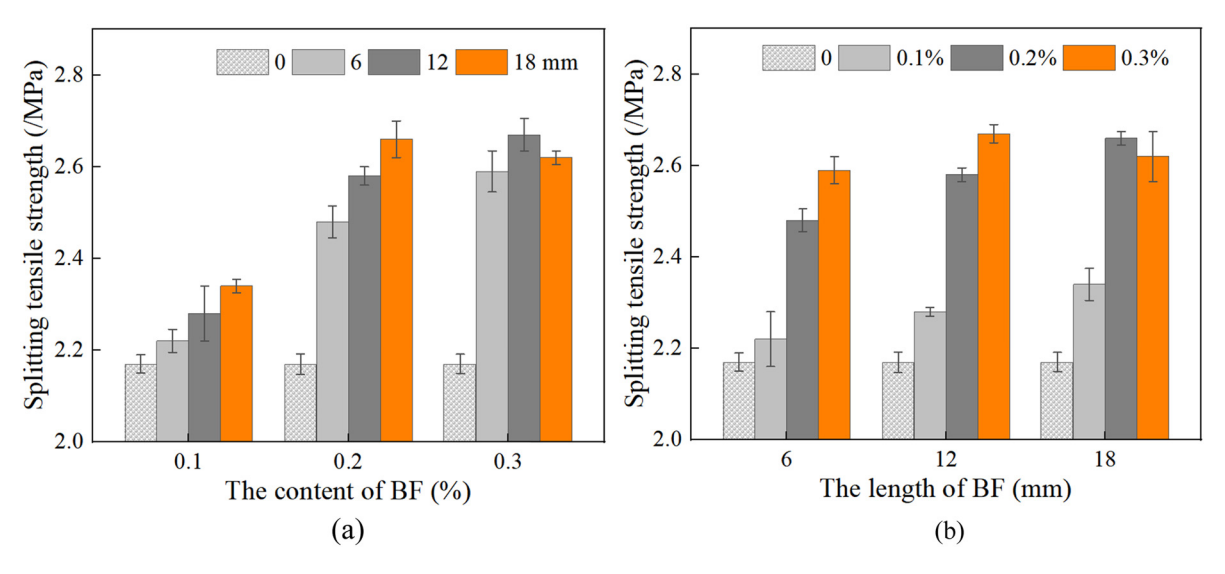
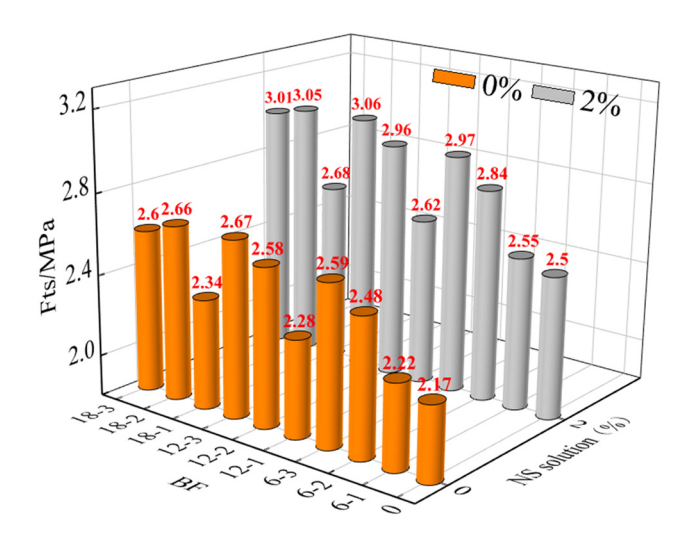


Figure 11: Effect of BF on the splitting tensile strength of RAC. (a) RAC with different BF contents. (b) RAC with different BF lengths.



**Figure 12:** The synergistic effect of NS and BF on the splitting tensile strength of RAC.

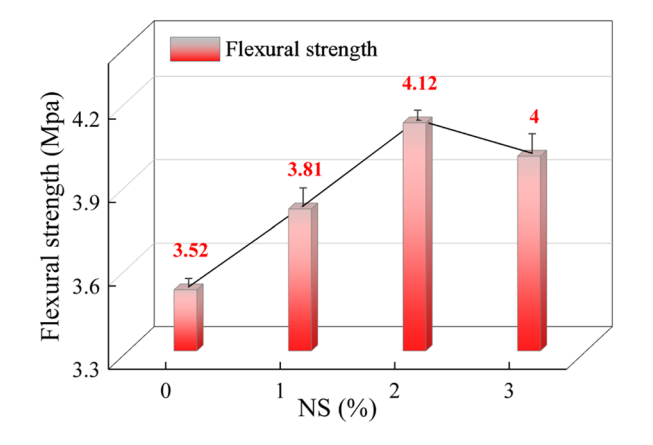


Figure 13: Effect of NS concentration on the flexural strength of RAC.

adding appropriate content of BF. Excessive BF leads to the superposition of fibers and poor adhesion between BF and cement mortar. As a result, there is weak ITZ in RAC, which produces defects easily when subjected to external forces. Similarly, when too short BF is added, the internal stress distribution of RAC is not concentrated, and cracks are prone to occur in the case of bending resistance. In addition, the effect of BF content on the flexural strength of RAC is greater than the length of BF based on the analysis of experimental data. When the content of BF is 0.2% and the lengths of BF are 12 and 18 mm, the improvement in the flexural strength is 28.13 and 32.10%, respectively.

For BF-reinforced RAC containing NS-modified RA, after RA is modified by NS, the strength of adhered mortar increases and a new ITZ is formed. The rough surface of RA is conducive to the uniform mixing of BF, which promotes the hydration reaction of RAC and makes the flexural strength develop rapidly. To sum up, adding an appropriate amount of BF and NS can greatly promote the flexural strength of RAC. As shown in Figure 15, when the concentration of NS is 2% and the length and content of BF are 12 mm and 0.2%, the flexural strength is increased by 54.55% compared with the unmodified RAC.

#### 3.6 Failure mode of RAC

#### 3.6.1 Failure mode of compressive strength specimen

Generally speaking, three failure forms occur when testing the compressive strength of concrete specimens, including

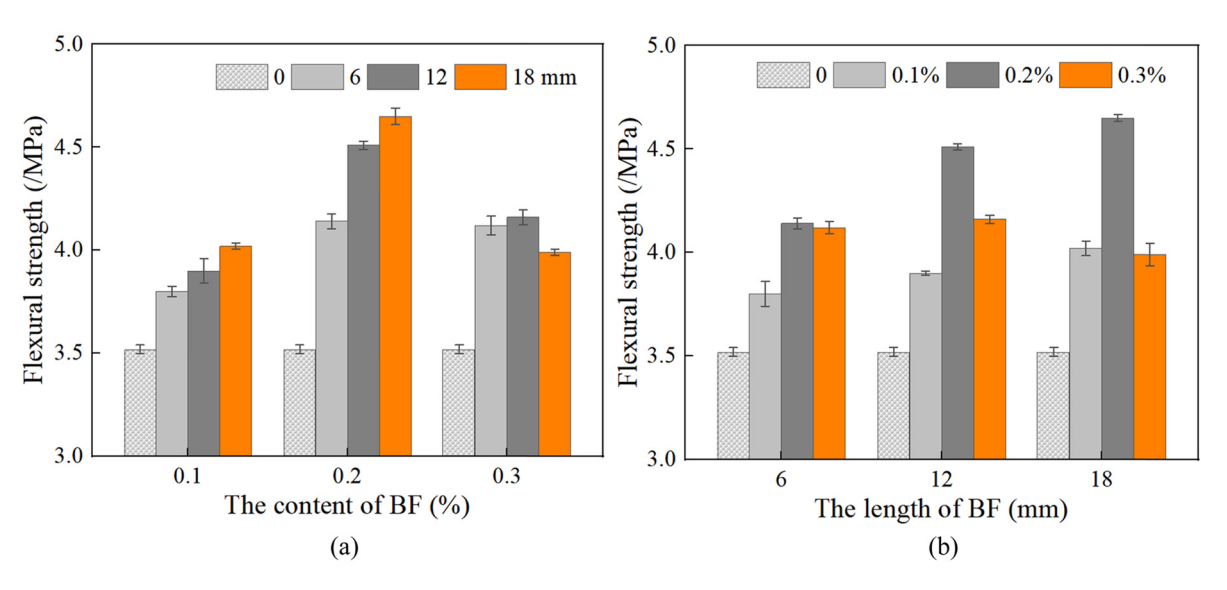
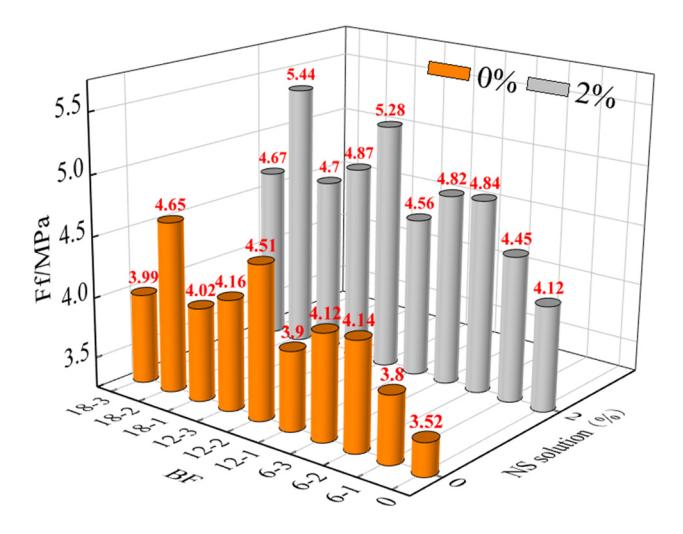


Figure 14: Effect of BF on the flexural strength of RAC. (a) RAC with different BF contents. (b) RAC with different BF lengths.



**Figure 15:** The synergistic effect of NS and BF on the flexural strength of RAC.

the bond failure between aggregate and cement mortar, the splitting failure of aggregate, and the tensile or shear failure of cement mortar. According to Figure 16(a) and (b), the damage form of RAC modified by NS is similar to that of ordinary RAC, and the damage generally occurs at the bond between RA and cement mortar, which is weaker

than that of ordinary RAC. As shown in Figure 16(c), the damage degree of the specimen is obviously weakened, the local drop phenomenon on the surface is obviously weakened, and the width and number of vertical cracks are obviously reduced. Figure 16(d) shows the compressive failure of BF-reinforced RAC containing NS-modified RA. At this time, the transverse and longitudinal deformation of RAC is obviously weakened under load, and the specimen maintains good integrity. Besides, Figure 17 shows that the compression failure of RAC goes through three processes. First, in the elastic stage, there is no crack on the surface of the RAC. Second, in the loading stage, in the surface perpendicular to the compression surface, many vertical cracks gradually appears when the peak load is reached. Third, in the failure stage, the surface crack gradually increases and develops from the outside to the inside until it is completely destroyed.

#### 3.6.2 Failure mode of splitting tensile specimen

The phenomenon of splitting tensile of RAC is basically the same as that of NAC, and the failure pattern of the specimen is shown in Figure 18(a). There is a fine crack

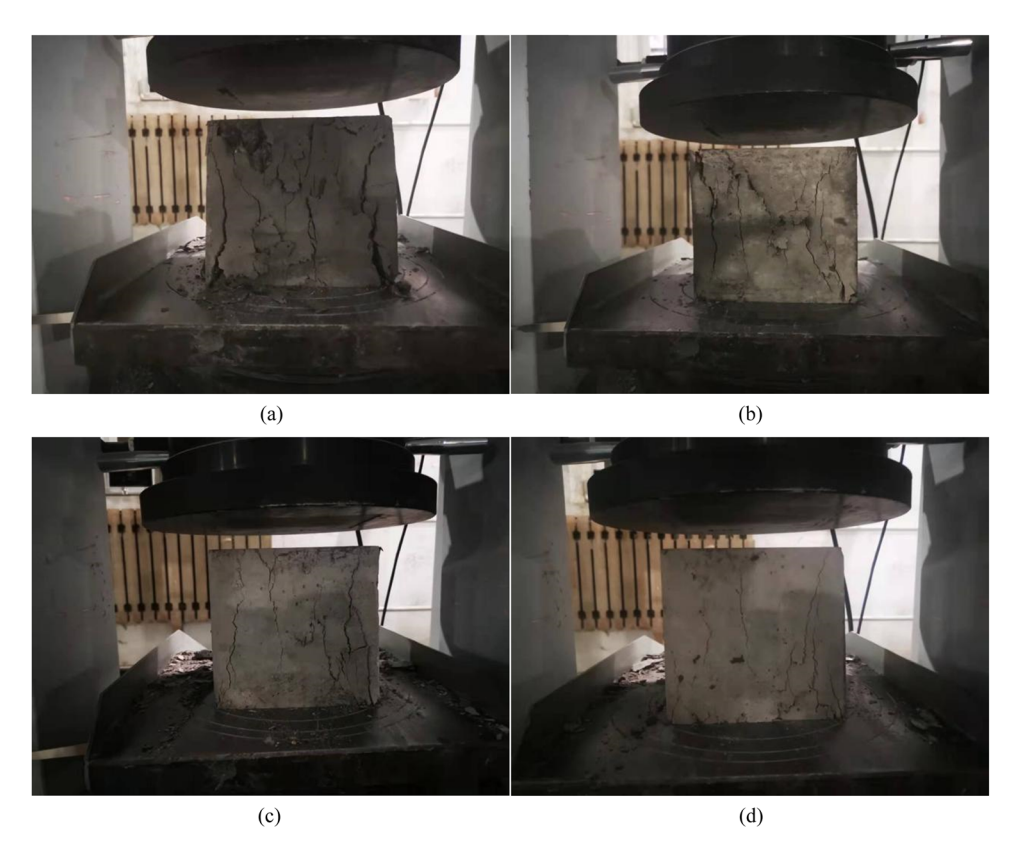


Figure 16: Cubic compression failure modes of RAC. (a) NSOBFO, (b) NS2BFO, (c) NSOBF12-2, (d) NS2BF12-2.

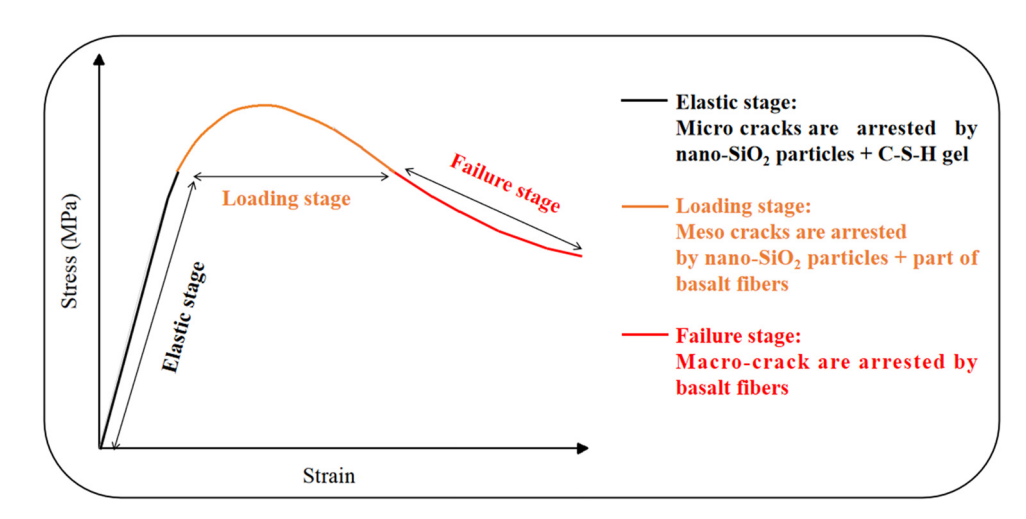


Figure 17: Multi-scale process of the compression failure of RAC.

near the cushion strip of the specimen, which expands rapidly through the top and bottom until the specimen is damaged. The time from loading to failure is very short, and the failure is a typical brittle failure. The main difference between the two is that most of the RAC fracture surface is located in the ITZ between new and old mortar. Figure 18(b) shows the failure pattern of RAC containing

NS-modified RA. It can be observed that the failure of the specimen is prolonged, and the crack width is lower than that of the ordinary RAC. The failure pattern of BFRAC is shown in Figure 18(c). The failure sections of the three are shown in Figure 18(d), compared with the ordinary RAC, the crack develops zigzag along the side of the specimen, and the width of the crack is smaller under the action of BF.

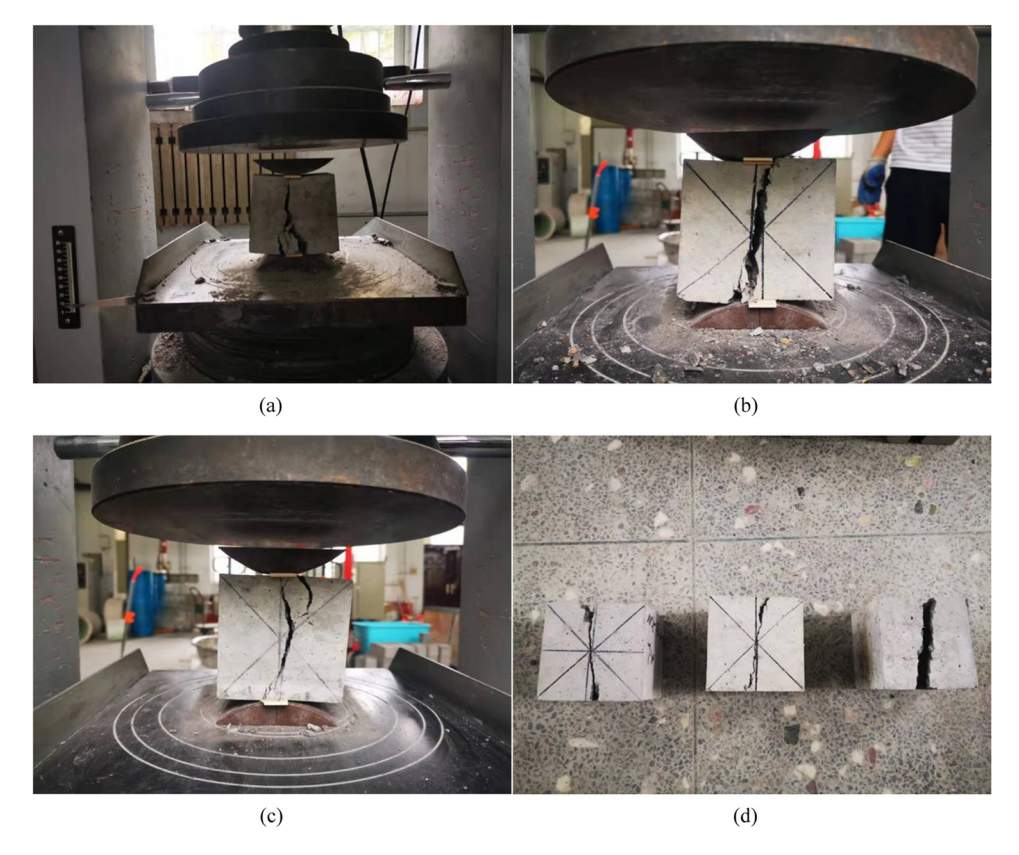


Figure 18: Splitting tensile failure modes of RAC. (a) RAC, (b) NSRAC, (c) BFRAC, (d) specimens after failure.

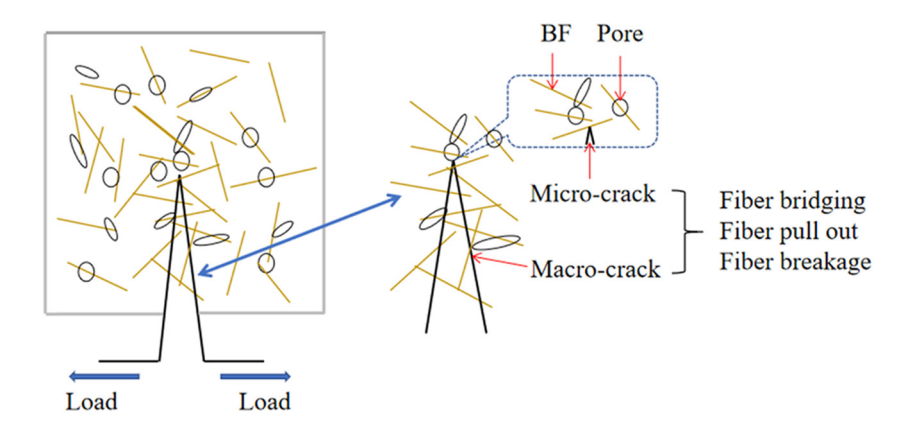


Figure 19: Multi-scale crack resistance process of BFRAC.

Figure 19 shows the multi-scale role of BF in the macro and micro-crack propagation process, reflecting the toughening and crack resistance mechanism of BF. After observing the damaged specimen, we can see that there are tortuous cracks on the specimen, and the sample has good integrity, which can be separated with the help of external force. Moreover, the fracture surface of BFRAC is curved rather than straight through, indicating that the fiber has an obvious anti-crack effect.

#### 3.6.3 Failure mode of flexural strength specimen

The flexural failure of RAC goes through three processes. First, in the elastic stage, there is no crack on the surface of the RAC. Second, after reaching the peak load, the bearing capacity of the specimen decreases until it breaks. As shown in Figure 20(a) and (b), the destruction process of ordinary RAC and RAC containing NS-modified RA is similar, and there is no obvious signal before the destruction occurs. When the ultimate load is reached,

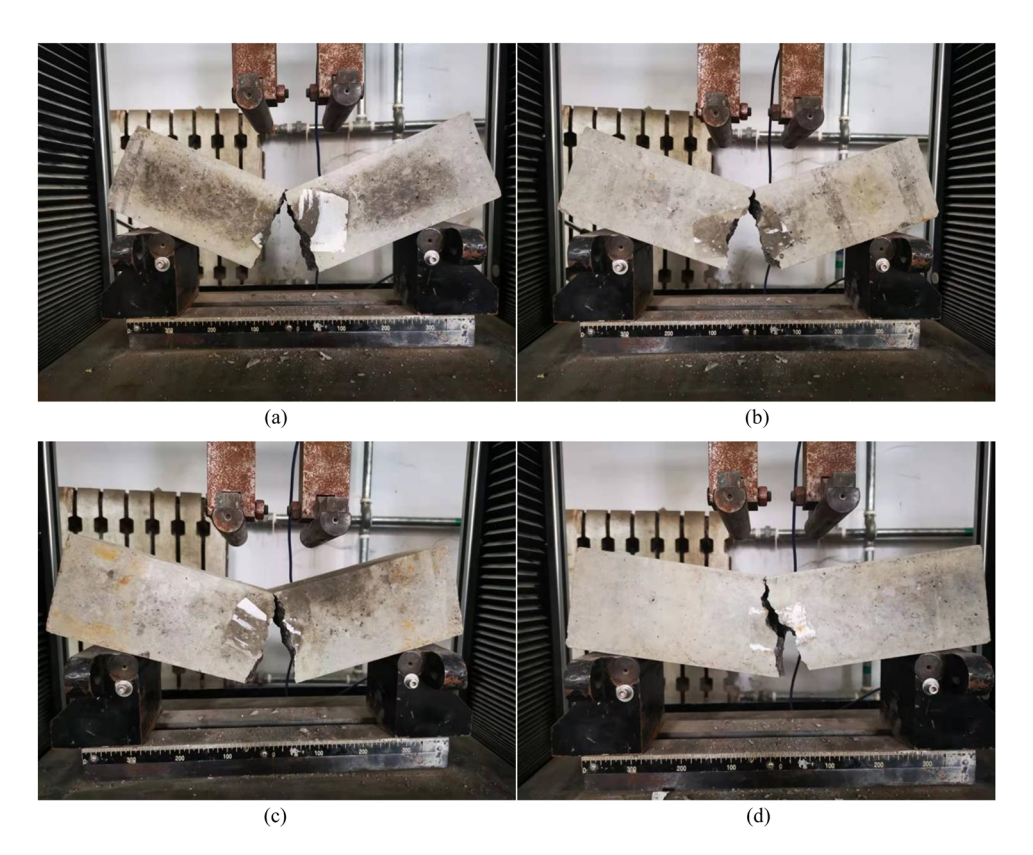


Figure 20: Flexural failure modes of RAC. (a) RAC, (b) NS2, (c) BF12-1, (d) BF12-2.

the specimen produces a loud noise and breaks, and the whole process is a typical brittle failure. According to Figure 20(c) and (d), the time from crack to fracture is slow, and it does not expand rapidly after the crack appears, and the rising rate of load reading is obviously slower than that of RAC. In addition, the fracture surface of the specimen is concave and convex, and RAC shows a certain toughness, which increases the ultimate load of the specimen, indicating that BF improves the bending performance of RAC. Figure 21 reflects the whole process of BFRAC from crack appearance to failure, studies the effect of BF on RAC pores and cracks, and shows the distribution of BF in cement matrix. At the same time, the fiber can also be regarded as a fine "steel bar" inside RAC, which directly reflects the crack resistance mechanism of BF.

# 4 Microstructure analysis of RAC

# 4.1 Micro-modification mechanism of nano-SiO<sub>2</sub>

ITZ is a weaker link in concrete and is a water-rich region. Compared with the cement matrix [64], ITZ has a high

water-cement ratio, large porosity, and more CH and  $3\text{CaO}\cdot\text{Al}_2\text{O}_3\cdot3\text{CaSO}_4\cdot32\text{H}_2\text{O}$  (AFt) and larger crystal particles [65]. The interface of RAC between the RA and cement mortar is clearer, and there are lots of pores and dispersed gel particles, thus forming a loose banded area [66]. These pores and harmful gel particles severely weaken the bonding properties of ITZ, which manifests as a decrease in the mechanical properties of RAC on a macroscopic scale [67,68]. Therefore, in this study, the modification mechanism of NS on the ITZ was analyzed and studied based on SEM measuring.

#### 4.1.1 Effect of nano-SiO<sub>2</sub> on ITZ strengthening of RAC

According to Figure 22(a), a band-like loose area between the cement mortar and the RA can be observed, and there are many pores on RA and obvious cracks in ITZs. In this case, some cement particles enter the aggregate and hydration reaction occurs, forming a lot of acicular AFt crystals and flake CH crystals. In turn, a dense shell is formed to prevent further hydration, resulting in a relatively loose structure of ITZ. Therefore, under the action of stress, the integrity of the ITZ is poor and penetration cracks are easy to appear. Through Figure 22(b), it can be found that the ITZ of RAC containing NS-modified RA is

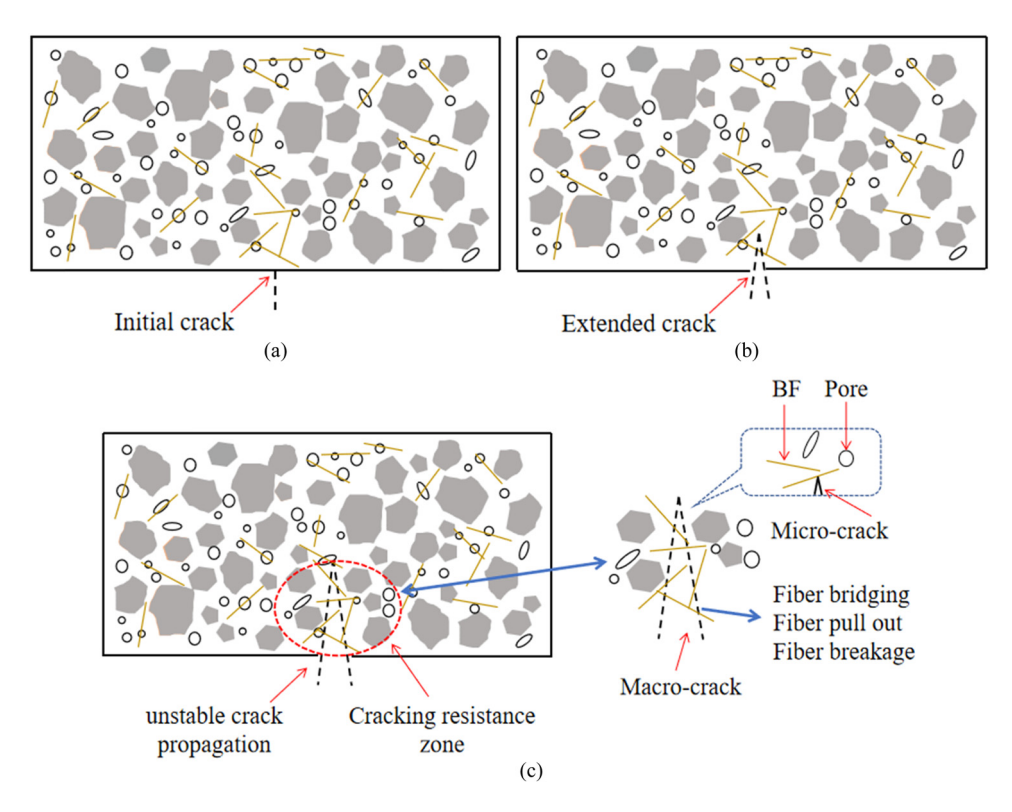


Figure 21: Flexural failure process of BFRAC. (a) Crack initiation process. (b) Crack propagation process. (c) Toughening and cracking resistance process.

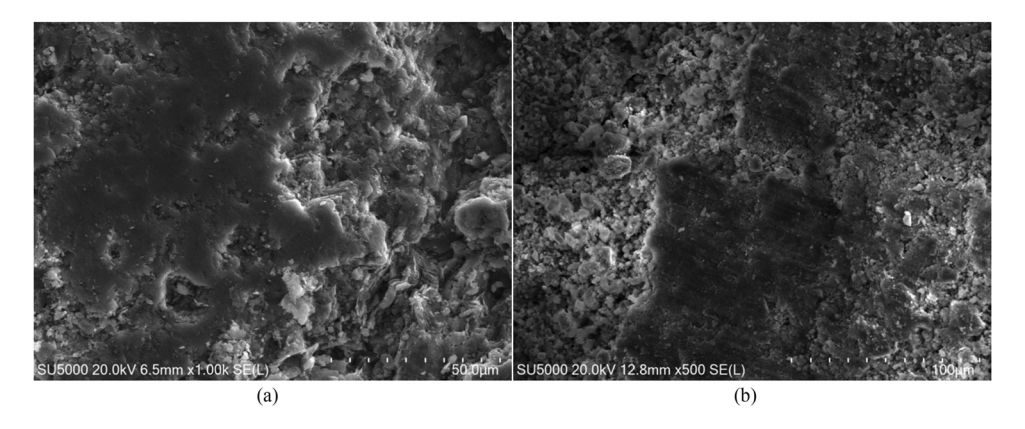


Figure 22: Micro-structure of the ITZ between RA and cement mortar before and after NS modification. (a) NS-0. (b) NS-2%.

relatively dense. There are obvious flocculent C–S–H gel formation and hydrate growth around ITZ, acicular and fibrous hydration products decrease, and bulk cluster hydration products increase. At the same time, it is found that there are no obvious cracks in ITZs, and the C–S–H gel is attached to the surface of RA, which improves the strength of RA and the integrity of new and old ITZ.

Figure 23(a) and (b) shows the micro-morphology of RAC cement paste before and after NS modification, respectively. From the observation of Figure 23(a), it can be seen that there are many unhydrated and dispersed cementitious particles on the surface of cement mortar, resulting in loose structure, poor compactness, and obvious cracks and holes. The existence of these defects causes serious damage to the mechanical properties of RAC. In addition, the existence of adhered mortar leads to a crystal enrichment layer formed by AFt and CH in RAC. Through Figure 23(b), it can be found that the hydration products around the modified coarse aggregate develop well, and the C–S–H gel can be observed obviously around the pores and macro-cracks in RAC. Furthermore,

the cement hydration mortar inside the specimen is very dense, the crack width becomes narrow, and the unhydrated C-S-H gel is glued together to form a dense continuous phase with high strength and density.

In summary, for RAC containing NS-modified RA, some CH crystals in ITZ are consumed and C-S-H gel is formed padding the pores of adhered mortar, which effectively reduces the content of CH crystal. Meanwhile, the generated C-S-H gel can effectively improve the structure of ITZ.

#### 4.1.2 Effect of nano-SiO2 on micro-structure of RA

Figure 24 shows the micro-morphology of RA based on SEM. It can be observed from Figure 24(a) that there are a large number of holes in the unmodified RA, there are a large number of AFt and CH crystals around the pores, and the structure of RA is loose. From Figure 24(b), it can be found that the pores of RA are reduced, and they are filled with more neat and dense C–S–H gel. In addition,

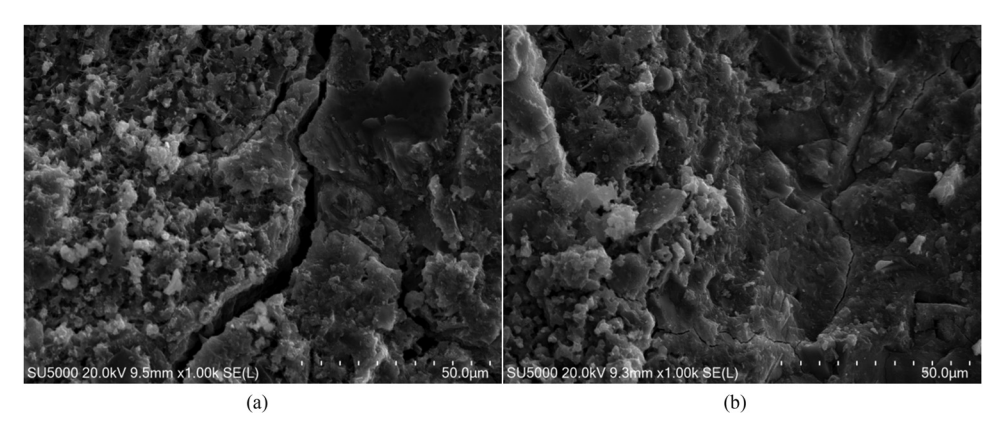


Figure 23: Micro-morphology of the cement mortar of RAC before and after NS modification. (a) NS-0. (b) NS-2%.

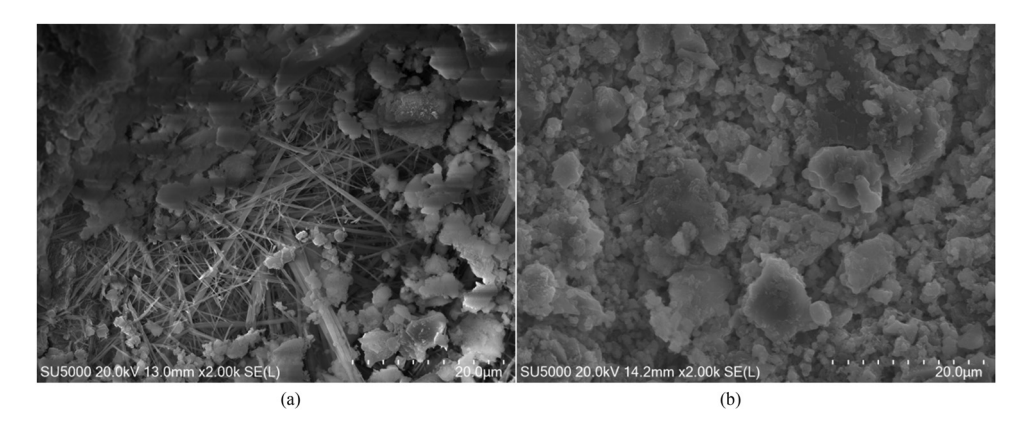


Figure 24: Micro-morphology of RA before and after NS modification. (a) NS-0, (b) NS-2%.

the gels are tightly packed, the number of needle-like AFt and CH crystals becomes less, and the structure of RA becomes dense. Macroscopically, it is shown that the basic physical properties of RA are improved, which in turn has an effective improvement on the mechanical properties and durability of RAC. NS has the characteristics of small particle size and high chemical activity, so it is easy to combine with other atoms. After RA was soaked in NS solution, NS particles reacted continuously with CH crystals in RA. The low-strength CH crystals were transformed

into high-strength C-S-H flocculent gels, which were filled in the internal pores of RA and attached to the mortar, so that the structure of RA became compact.

#### 4.2 Micro-modification mechanism of BF

According to Figure 25(a)–(c), with the change in the content of BF from 0.1 to 0.3%, the internal structure of RAC goes through a process from loose to dense and then

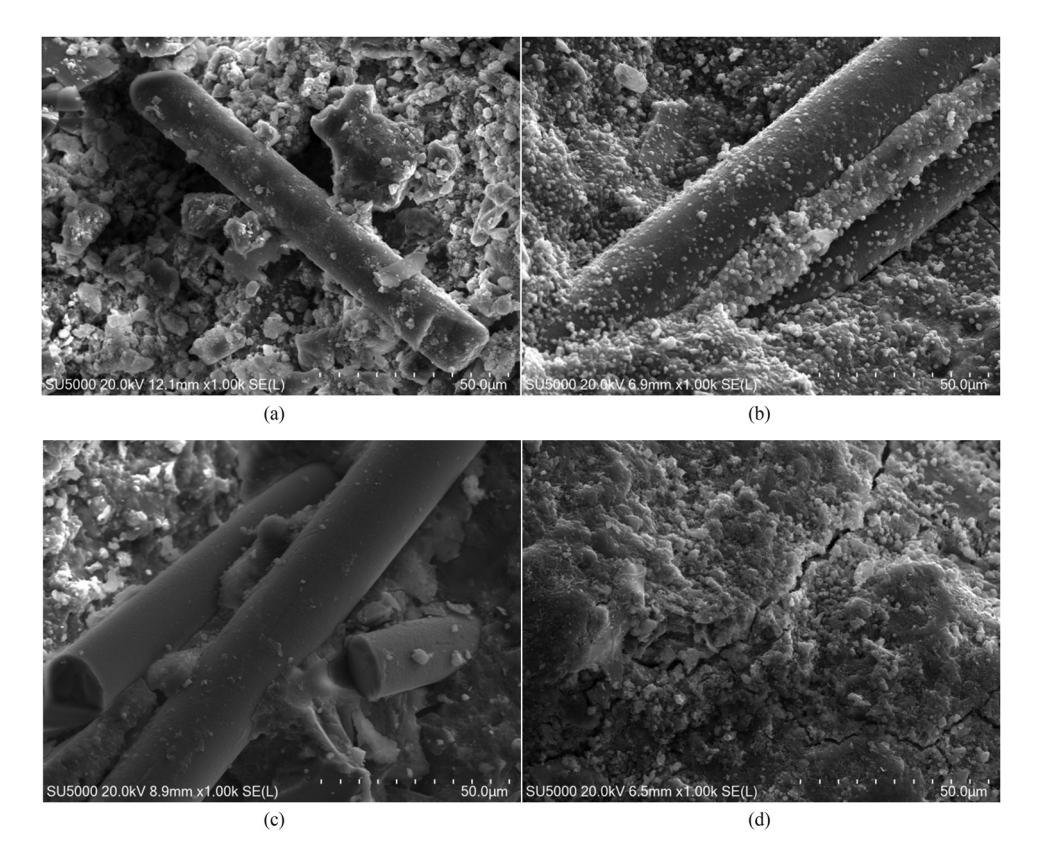


Figure 25: The bonding between BF and cement matrix under SEM measuring. (a) BF12-0.1%, (b) BF12-0.2%, (c) and (d) both show BF12-0.3%, which does not need to be modified here.

to loose. When the content of BF was 0.1%, it was observed that the fiber was wrapped by a small amount of white gel, and the internal structure of RAC was improved. But at this time, due to the small number of fibers, there were still many defects in the concrete. When the content of BF was 0.2%, a large amount of white gel was observed on the surface of BF, and it was closely connected with the cement matrix. The staggered distribution of BF in cement mortar plays the bridging role of BF, which makes the spatial structure of RAC compact. When the content of BF was 0.3%, a certain degree of separation between BF and matrix was observed, which made the interface layer between cement matrix and BF more loose and white gel reduced. Too many fibers were unevenly dispersed and prone to agglomeration, resulting in more defects and cracks in RAC, and the spatial layout of the matrix became sparse. Figure 25(d) shows the microscopic morphology of the cement matrix in the RAC when the content of BF is 0.3%. It can be observed that relatively obvious pores and cracks are distributed in the matrix, and the compactness of the internal structure is poor.

Due to the uniform distribution of BF, the microstructure of concrete is compact, the stress distribution of internal structure is improved, and the internal pore structure is optimized. In addition, BF effectively suppresses the phenomenon of stress concentration, and the fibers traversing the crack continue to bear the load after the concrete is damaged, preventing the crack development and penetration and preventing the premature failure of the weak surface. In turn, it improves the ability of RAC to resist static damage, which shows the relative improvement of splitting tensile strength. However, when the content of BF is too high, BF agglomerates and a large area of weak ITZ between the cement matrix and fiber will be produced, which will make the internal structure of concrete to exhibit loose plastic characteristics. At this

time, the gain effect of BF on concrete is gradually offset by the benefit-reducing effect, which makes the mechanical strength of BFRAC increase at first and then decrease.

### 4.3 Micro-mechanism of synergistic strengthening of RAC by NS and BF

In the presence of appropriate amount of NS, the high activity of NS greatly accelerates the reaction rate between NS and irregular CH crystals. At the same time, a lot of hydration heat is released, which further promotes the hydration reaction of cement and produces a large number of C-S-H gels in the RAC. The above reactions enhance the compactness of the internal structure of cement matrix, so the addition of NS is beneficial to the increase in RAC strength.

After adding appropriate content of BF alone, when RAC is subjected to external tension, the weakest ITZ in the coagulation structure is destroyed first, and the failure form of BF is shown in Figure 26. The BF across the ITZ can effectively avoid and reduce the occurrence of microcracks, while the supporting system formed by the randomly distributed BF plays a role in further preventing the extension and expansion of micro-cracks. Zhang et al. [46] obtained similar results by SEM measuring.

As shown in Figure 27, based on SEM and EDS measuring, the analysis was carried out at the ITZ of two groups of specimens of NS0BF12-2 and NS2BF12-2. According to the EDS analysis, the main chemical elements of the hydration products attached to the surface of BF in BFRAC were Al, Si, Ca, and O, indicating that the hydration products were mainly C-S-H gel. When the content of NS is 0 and 2%, respectively, the atomic percentage of Si in the latter is significantly higher than that of the former, and the Ca/Si

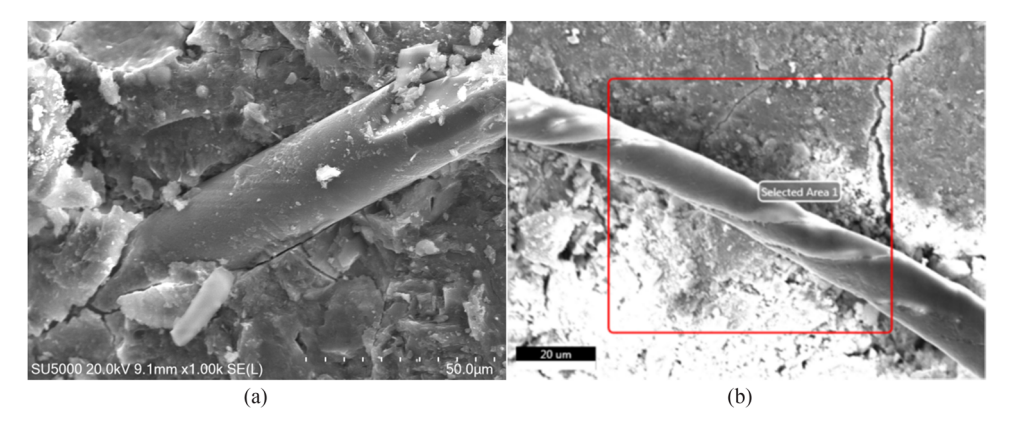


Figure 26: The failure form of BF. (a) Drawing failure and (b) torsional failure.

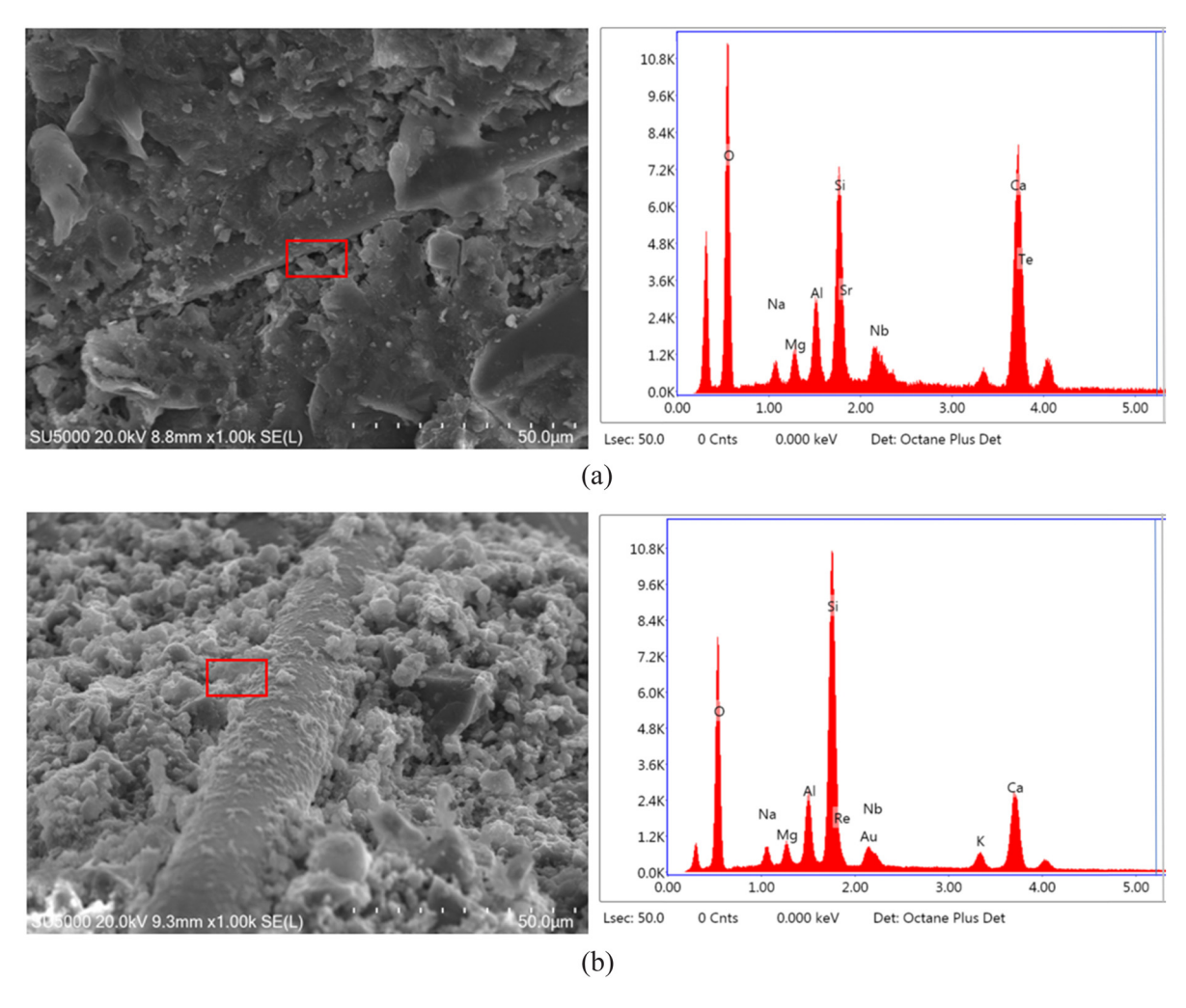


Figure 27: SEM-EDS analysis of BF-reinforced RAC containing NS-modified RA. (a) NS0BF12-2, (b) NS2BF12-2.

is lower than the former. It shows that the addition of NS increases the C–S–H gel content of the ITZ between BF and matrix, indicating that the cement mortar around the fiber is well hydrated and there is no large amount of CH aggregation. For BF-reinforced RAC containing NS-modified RA, the flocculent C–S–H gel formed by the reaction can be closely packed, which enhances the bond between matrix and BF, and effectively promotes the performance of ITZ. The result validates the microscopic mechanism of BF-reinforced RAC containing NS-modified RA.

#### 5 Conclusion

In this study, the length and content of BF, the concentration of NS solution, the BF-reinforced RAC containing NSmodified RA, and the micro-strengthening mechanism were studied. The main conclusions are as follows:

- 1) 2% is determined to be the best soaking concentration of NS through the comparative analysis of the soaking effect. The water absorption and crushing index of modified RA decreased by 28.53 and 29.85%, respectively. The strengthening mechanism of NS on RA can be summarized as filling effect, high chemical activity, nucleation, and optimization of ITZ.
- 2) The content of BF is the main factor affecting the mechanical properties of RAC, and the optimum content is 0.2%. The length of BF has little effect on the compressive properties of RAC, but the increase in the length of BF can appropriately enhance the splitting tensile and flexural properties.
- 3) For BF-reinforced RAC containing NS-modified RA, the optimal content of NS and BF is 2% and 12–0.2%, respectively. The compressive strength, splitting tensile strength, and flexural strength of strengthened RAC are improved in varying degrees, and the corresponding strength is increased by 34.28, 40.55, and 54.5%, respectively.

4) Based on SEM and EDS measuring, NS can effectively improve the pores and cracks of the internal structure of RA, reduce the calcium-silicon ratio of the ITZ between BF and cement matrix, and enhance the bonding of the ITZ. The rough surface of RA is beneficial to the distribution of BF, and the proper content of BF makes the spatial structure of RAC compact.

Author contributions: All authors have accepted responsibility for the entire content of this manuscript and approved its submission.

Conflict of interest: The authors state no conflict of

# 6 Recommendations for future work

In this study, the mechanical properties of RA and RAC were studied from macro-and microcosmic scales, and the micro strengthening mechanism of nano-SiO2, BF, and their synergistic effect on RAC were proposed. However, there are some recommendations for future work:

- 1) At present, in most studies, the performance of RAC was improved by adding modified materials, but there are few studies on the influence of loading rate, specimen size, and condition (dry and wet), and moisture condition of the RA particles on the performance of RAC.
- 2) At present, the utilization rate of recycled fine aggregate with particle size less than 4.75 mm is not high enough. Therefore, using waste mortar and fine aggregate to make green cementitious material instead of cement, and preparing RAC with high quality is an
- 3) The mix design of RAC is mostly based on the code of ordinary concrete; the high water absorption of RA is not taken into account, and the research on the mix design method of BFRAC should be studied further.

Acknowledgments: The authors would like to acknowledge the financial support received from National Natural Science Foundation of China (Grant No. 51878623 and U2040224), Natural Science Foundation of Henan (Grant No. 212300410018), and Program for Innovative Research Team (in Science and Technology) in University of Henan Province of China (Grant No. 20IRTSTHN009).

**Funding information:** The authors would like to acknowledge the financial support received from National Natural Science Foundation of China (Grant No. 51878623 and U2040224), Natural Science Foundation of Henan (Grant No. 212300410018), and Program for Innovative Research Team (in Science and Technology) in University of Henan Province of China (Grant No. 20IRTSTHN009).

#### References

- Verian KP, Ashraf W, Cao Y, Properties of recycled concrete aggregate and their influence in new concrete production. Resour Conserv Recycl. 2018;133:30-49.
- Shi C, Li Y, Zhang J, Li W, Chong L. Performance enhancement of recycled concrete aggregate-a review. J Clean Prod. 2016;112:466-72.
- [3] Wang J, Zhang J, Cao D, Dang H, Ding B. Comparison of recycled aggregate treatment methods on the performance for recycled concrete. Constr Build Mater. 2020;234:117366.
- Zaetang Y, Sata V, Wongsa A, Chindaprasirt P. Properties of pervious concrete containing recycled concrete block aggregate and recycled concrete aggregate. Constr Build Mater. 2016;111:15-21.
- Zheng Y, Zhang Y, Zhang P. Methods for improving the dur-[5] ability of recycled aggregate concrete: A review. J Mater Sci Technol. 2021;15:6367-86.
- Lu B, Shi C, Cao Z, Guo M, Zheng J. Effect of carbonated coarse recycled concrete aggregate on the properties and microstructure of recycled concrete. J Clean Prod. 2019;233:421-8.
- [7] Chen S, Xing C, Zhao M, Zhang J, Wang L. Recycled aggregate pervious concrete: Analysis of influence of water-cement ratio and fly ash under single action and optimal design of mix proportion. J Renew Mater. 2022;10(3):799-819.
- Xuan D, Zhan B, Poon CS. Durability of recycled aggregate concrete prepared with carbonated recycled concrete aggregates. Cem Concr Compos. 2017;84:214-21.
- Cantero B, Bravo M, de Brito J, Del Bosque IS, Medina C. Mechanical behaviour of structural concrete with ground recycled concrete cement and mixed recycled aggregate. J Clean Prod. 2020;275:122913.
- [10] Bonifazi G, Palmieri R, Serranti S. Evaluation of attached mortar on recycled concrete aggregates by hyperspectral imaging. Constr Build Mater. 2018;169:835-42.
- Fan Y, Xiao J, Tam VW. Effect of old attached mortar on the [11] creep of recycled aggregate concrete. Struct Concr. 2014;15(2):169-78.
- [12] Xuan D, Zhan B, Poon CS. Assessment of mechanical properties of concrete incorporating carbonated recycled concrete aggregates. Cem Concr Compos. 2016;65:67-74.
- Gupta PK, Khaudhair ZA, Ahuja AK. A new method for proportioning recycled concrete. Struct Concr. 2016;17(4):677-87.
- [14] Leite MB, Monteiro PJM. Microstructural analysis of recycled concrete using X-ray microtomography. Cem Concr Res.
- [15] Algarni AS, Abbas H, Al-Shwikh KM, Al-Salloum YA. Treatment of recycled concrete aggregate to enhance concrete performance. Constr Build Mater. 2021;307:124960.

- [16] Zega CJ, Villagrán-Zaccardi YA, Di, Maio AA. Effect of natural coarse aggregate type on the physical and mechanical properties of recycled coarse aggregates. Mater Struct. 2010;43(1):195-202.
- [17] Zhao J, Zhang B, Xie J, Wu Y, Wang Z. Effects of nano-SiO<sub>2</sub> modification on rubberised mortar and concrete with recycled coarse aggregates. Nanotechnol Rev. 2022;11(1):473-96.
- [18] Liu C, Lv Z, Xiao J, Xu X, Nong X. On the mechanism of Cldiffusion transport in self-healing concrete based on recycled coarse aggregates as microbial carriers. Cem Concr Compos. 2021;124:104232.
- [19] Wang L, Lu X, Liu L, Xiao J, Zhang G, Guo F, et al. Influence of MgO on the hydration and shrinkage behavior of low heat Portland cement-based materials via pore structural and fractal analysis. Fractal Fract. 2022;6(1):40.
- [20] Wang L, Luo R, Zhang W, Jin M, Tang S. Effects of fineness and content of phosphorus slag on cement hydration, permeability, pore structure and fractal dimension of concrete. Fractals. 2021;29(2):2140004.
- [21] Zheng Y, Zhuo J, Zhang P. A review on durability of nano-SiO<sub>2</sub> and basalt fiber modified recycled aggregate concrete. Constr Build Mater. 2021;304:124659.
- [22] Chen S, Zhao Y, Bie Y. The prediction analysis of properties of recycled aggregate permeable concrete based on back-propagation neural network. J Clean Prod. 2020;276:124187.
- [23] Liu G, Li Q, Song J, Wang L, Liu H, Guo Y, et al. Quantitative analysis of surface attached mortar for recycled coarse aggregate. Materials. 2022;15(1):257.
- [24] Han Q, Zhang P, Wu J, Jing Y, Zhang D, Zhang T. Comprehensive review of the properties of fly ash-based geopolymer with additive of nano-SiO<sub>2</sub>. Nanotechnol Rev. 2022;11(1):1478-98.
- [25] Zhang X, Zhang P, Wang T, Zheng Y, Qiu L, Sun S. Compressive strength and anti-chloride ion penetration assessment of geopolymer mortar merging PVA fiber and nano-SiO2 using RBF-BP composite neural network. Nanotechnol Rev. 2022;11(1):1181-92.
- [26] Gao C, Huang L, Yan L, Kasal B, Li W, Jin R, et al. Compressive performance of fiber reinforced polymer encased recycled concrete with nanoparticles. J Mater Res Technol. 2021:14:2727-38.
- [27] Younis KH, Mustafa SM. Feasibility of using nanoparticles of SiO<sub>2</sub> to improve the performance of recycled aggregate concrete. Adv Mater Sci Eng. 2018;2018:2018-111.
- [28] Younis KH. Nano-Silica modified recycled aggregate concrete: Mechanical properties and microstructure. Eurasian J Sci Eng. 2018;3(3):167-76.
- [29] Mukharjee BB, Barai SV. Mechanical and microstructural characterization of recycled aggregate concrete containing silica nanoparticles. J Sustain Cem-Based. 2017;6(1):37-53.
- [30] Ying J, Zhou B, Xiao J. Pore structure and chloride diffusivity of recycled aggregate concrete with nano-SiO<sub>2</sub> and nano-TiO<sub>2</sub>. Constr Build Mater. 2017;150:49-55.
- [31] Zheng Y, Zhang Y, Zhuo J, Zhang P, Kong W. Mechanical properties and microstructure of nano-strengthened recycled aggregate concrete. Nanotechnol Rev. 2022;11(1):1499-510.
- [32] Zhang P, Wang K, Wang J, Guo J, Hu S, Ling Y. Mechanical properties and prediction of fracture parameters of geopolymer/alkali-activated mortar modified with PVA fiber and nano-SiO<sub>2</sub>. Ceram Int. 2020;46(12):20027-37.

- [33] Gao Z, Zhang P, Wang J, Wang K, Zhang T. Interfacial properties of geopolymer mortar and concrete substrate: Effect of polyvinyl alcohol fiber and nano-SiO<sub>2</sub> contents. Constr Build Mater. 2022;315:125735.
- [34] Zeng W, Zhao Y, Zheng H, Poon CS. Improvement in corrosion resistance of recycled aggregate concrete by nano silica suspension modification on recycled aggregates. Cem Concr Compos. 2020;106(103476):103476.
- [35] Gao Z, Zhang P, Guo J, Wang K. Bonding behavior of concrete matrix and alkali-activated mortar incorporating nano-SiO<sub>2</sub> and polyvinyl alcohol fiber: Theoretical analysis and prediction model. Ceram Int. 2021;47(22):31638-49.
- [36] Li W, Luo Z, Long C, Wu C, Duan WH. Effects of nanoparticle on the dynamic behaviors of recycled aggregate concrete under impact loading. Mater Des. 2016;112:58-66.
- [37] Zhang P, Wang K, Wang J, Guo J, Ling Y. Macroscopic and microscopic analyses on mechanical performance of metakaolin/ flyash based geopolymer mortar. J Clean Prod. 2021;294:126193.
- [38] Shaikh F, Chavda V, Minhaj N, Arel HS. Effect of mixing methods of nano silica on properties of recycled aggregate concrete. Struct Concr. 2018;19(2):387-99.
- [39] Zhang H, Zhao Y, Meng T, Shah SP. Surface treatment on recycled coarse aggregates with nanomaterials. J Mater Civ Eng. 2016;28(2):4015094.
- [40] Fu Q, Xu W, Li D, Li N, Niu D, Zhang L, et al. Dynamic compressive behaviour of hybrid basalt-polypropylene fibre-reinforced concrete under confining pressure: Experimental characterisation and strength criterion. Cem Concr Compos. 2021;118:103954.
- [41] Wen C, Zhang P, Wang J, Hu S. Influence of fibers on the mechanical properties and durability of ultra-high-performance concrete: A review. J Build Eng. 2022;52:104370.
- [42] Liew KM, Akbar A. The recent progress of recycled steel fiber reinforced concrete. Constr Build Mater. 2020;232:117232.
- [43] Wang L, Guo F, Yang H, Wang Y, Tang S. Comparison of fly ash, PVA fiber, MgO and shrinkage-reducing admixture on the frost resistance of face slab concrete via pore structural and fractal analysis. Fractals. 2021;29(2):2140002.
- [44] Wang K, Zhang P, Guo J, Gao Z. Single and synergistic enhancement on durability of geopolymer mortar by polyvinyl alcohol fiber and nano-SiO<sub>2</sub>. J Mater Res Technol. 2021;15:1801-14.
- [45] Qin Y, Li M, Li Y, Ma W, Xu Z, Chai J, et al. Effects of nylon fiber and nylon fiber fabric on the permeability of cracked concrete. Constr Build Mater. 2021;274:121786.
- [46] Zhang C, Wang Y, Zhang X, Ding Y, Xu P. Mechanical properties and microstructure of basalt fiber-reinforced recycled concrete. J Clean Prod. 2021;278:123252.
- [47] Khandelwal S, Rhee KY. Recent advances in basalt-fiber-reinforced composites: Tailoring the fiber-matrix interface. Compos B Eng. 2020;192:108011.
- [48] Qin Y, Zhang X, Chai J, Xu Z, Li S. Experimental study of compressive behavior of polypropylene-fiber-reinforced and polypropylene-fiber-fabric-reinforced concrete. Constr Build Mater. 2019;194:216-25.
- [49] Nihat K. Abrasion resistance and fracture energy of concretes with basalt fiber. Constr Build Mater. 2014;50:95-101.
- [50] Li S, Zhang Y, Chen W. Bending performance of unbonded prestressed basalt fiber recycled concrete beams. Eng Struct. 2020;221:110937.

**DE GRUYTER** 

- [51] Fang S, Hong H, Zhang P. Mechanical property tests and strength formulas of basalt fiber reinforced recycled aggregate concrete. Materials. 2018;11:1851.
- [52] Katkhuda H, Shatarat N. Improving the mechanical properties of recycled concrete aggregate using chopped basalt fibers and acid treatment. Constr Build Mater. 2017;140:328-35.
- [53] Zheng Y, Zhang P, Cai Y, Jin Z, Moshtagh E. Cracking resistance and mechanical properties of basalt fibers reinforced cementstabilized macadam. Compos B Eng. 2019;165:312-34.
- [54] Wang Y, Hughes P, Niu H, Fan Y. A new method to improve the properties of recycled aggregate concrete: Composite addition of basalt fiber and nano-silica. J Clean Prod. 2019;236:117602.
- [55] Hassani Niaki M, Fereidoon A, Ghorbanzadeh, Ahangari M. Experimental study on the mechanical and thermal properties of basalt fiber and nanoclay reinforced polymer concrete. Compos Struct. 2018;191:231-8.
- [56] Wang Y, Li S, Hughes P, Fan Y. Mechanical properties and microstructure of basalt fibre and nano-silica reinforced recycled concrete after exposure to elevated temperatures. Constr Build Mater. 2020;247(118561):118561.
- [57] Wei B, Song S, Cao H. Strengthening of basalt fibers with nano- $SiO_2$ -epoxy composite coating. Mater Des. 2011;32(8–9):4180–6.
- [58] Bian Y, Li Z, Zhao J, Wang Y. Synergistic enhancement effect of recycled fine powder (RFP) cement paste and carbonation on recycled aggregates performances and its mechanism. J Clean Prod. 2022;344:130848.
- Nepomuceno MC, Isidoro RA, Catarino JP. Mechanical perfor-[59] mance evaluation of concrete made with recycled ceramic coarse aggregates from industrial brick waste. Constr Build Mater. 2018;165:284-94.

- [60] Urkhanova LA, Lkhasaranov SA, Rozina VE, Buyanture SL. Fine Basalt-Fibrous-Concrete with Nano-Silica. Constr Mater. 2015;6:45-8.
- [61] Iyer P, Kenno SY, Das S. Mechanical properties of Fiber-Reinforced concrete made with basalt filament fibers. J Mater Civ Eng. 2015;27(11):4015015.
- [62] Kou S, Poon C, Etxeberria M. Influence of recycled aggregates on long term mechanical properties and pore size distribution of concrete. Cem Concr Compos. 2011;33(2):286-91.
- [63] Chen X, Kou S, Xing F. Mechanical and durable properties of chopped basalt fiber reinforced recycled aggregate concrete and the mathematical modeling. Constr Build Mater. 2021:298:123901.
- [64] Golewski GL. Evaluation of morphology and size of cracks of the Interfacial Transition Zone (ITZ) in concrete containing fly ash (FA). J Hazard Mater. 2018;357:298-304.
- [65] Golewski GL. An assessment of microcracks in the Interfacial Transition Zone of durable concrete composites with fly ash additives. Compos Struct. 2018;200:515-20.
- [66] Xiao J, Li W, Sun Z, Lange DA, Shah SP. Properties of interfacial transition zones in recycled aggregate concrete tested by nanoindentation. Cem Concr Compos. 2013;37:276-92.
- Zhan B, Xuan D, Poon CS, Scrivene KL. Characterization of [67] interfacial transition zone in concrete prepared with carbonated modeled recycled concrete aggregates. Cem Concr Res. 2020;136(106175):106175.
- [68] Bai W, Li W, Guan J, Wang J, Yuan C. Research on the mechanical properties of recycled aggregate concrete under uniaxial compression based on the statistical damage model. Materials. 2020;13(17):3765.